Solid State Ionics 326 (2018) 166–172

Contents lists available at ScienceDirect

Solid State Ionics

journal homepage: www.elsevier.com/locate/ssi

Electrical, structural, and thermal properties of succinonitrile-LiI-I_2 redox-mediator

Ravindra Kumar Gupta[a,*], Idriss Bedja[a], Ashraful Islam[b], Hamid Shaikh[c]

[a] Cornea Research Chair, Department of Optometry, College of Applied Medical Sciences, King Saud University, P.O. Box 10219, Riyadh 11433, Saudi Arabia
[b] National Institute for Materials Science (NIMS), Photovoltaic Materials Group, Sengen 1-2-1, Tsukuba 305-0047, Japan
[c] SABIC Polymer Research Center, Department of Chemical Engineering, College of Engineering, King Saud University, P.O. Box 800, Riyadh 11421, Saudi Arabia

ARTICLE INFO

Keywords:
Dye-sensitized solar cells
Succinonitrile
Electrical conductivity
Ionic transference number
Vibrational spectroscopy

ABSTRACT

We synthesized a solid I^-/I_3^--based redox-couple electrolyte using a mixture of succinonitrile, LiI and I_2. An increase of LiI to succinonitrile mole ratio (x) up to 2.5% led to a fast rise in the electrical conductivity ($\sigma_{25°C}$) of the electrolytes. Further increase in x slowly increased the $\sigma_{25°C}$-value. The composition with $x = 5\%$ achieved the highest $\sigma_{25°C}$-value ($\sim 1.6 \times 10^{-3}\,S\,cm^{-1}$) and was referred to as the optimum conducting composition (OCC) of the electrolytes. Also, an increase of x led to a decrease of the melting temperature of the electrolytes as suggested by the $\log\sigma - T^{-1}$ study and ascertained by the differential scanning calorimetry study. The $\log\sigma - T^{-1}$ study showed a linear trend before and after the melting temperature, and the activation energy increased with increasing x-value. The electrical and thermal properties were explained using the vibrational spectroscopy study. The ionic transference number measurement showed that the electrolytes with $x = 4$ and 5% are predominantly ionic in nature.

1. Introduction

Renewable energy sources are currently highly demanding because of the environmental issues. The high rise of levels of greenhouse gases and pollution especially in developed and developing countries is leading to a potential mass destruction of the humankind through negative environmental effects. One of the renewable energy sources, the solar cell, is highly useful in a country like Saudi Arabia, where solar irradiance is quite high [1]. The dye-sensitized solar cell (DSSC), a third-generation solar cell, offers simple cell structure and cost-effectiveness in materials and manufacturing as compared to other solar cells [2]. Short energy payback time (< 1 year), enhanced performance under real outdoor conditions and capturing of light from all angles of the incident are some of the interesting features of the DSSCs. In the conventional DSSC, an I^-/I_3^--based redox-couple liquid electrolyte is used for dye regeneration at the working electrode (WE; mesoporous TiO_2 layer) [2,3]. The dye regeneration occurs via oxidation of I^- producing I_3^-. The reduction of I_3^- into I^- occurs at the counter electrode (platinum layer). A fast diffusion of redox-couple is required for the efficient cell operation [3]. At present, the highest cell efficiency, $\eta \sim 11.1\%$, is reported for the liquid electrolyte: 0.6 M dimethyl propyl imidazolium iodide, 0.1 M LiI, 0.05 M iodine, and 0.5 M tert-butylpryidine (TBP) in acetonitrile [4]. The mixture, LiI-I_2 produces I^-/I_3^--redox-couple in the solution. The additive, TBP generally helps to increase the open circuit voltage of the cell by shifting the WE's conduction band towards higher energy. A use of imidazolium ionic liquid helps to increase the electrical conductivity and decrease the evaporation rate of the acetonitrile. A use of liquid electrolyte makes the cell prone to leakage of solvent especially at elevated operating temperature conditions due to the internal pressure. It also creates scale-up problem of manufacturing. The cell requires hermetic sealing too. Therefore, a solid electrolyte is required to meet the harsh environmental conditions as observed in gulf countries. For a review, see references, [2,3,5].

Succinonitrile (SN; N≡C−CH_2−CH_2−C≡N) is a non-ionic and low-molecular-weight plastic crystal, which has a plastic crystal phase between −38 °C (crystal to plastic crystal phase transition temperature, T_{pc}) and 58 °C (melting temperature, T_m) allowing a high molecular diffusivity via increasing concentration of trans isomers and molecular jumps from one diagonal position of the cubic structure to another [6–8]. Because of its low T_m-value, high dielectric constant (~55) and waxy nature, succinonitrile also acts as a solid solvent/plasticizer to prepare redox-couple solid or gel electrolytes for dye-sensitized solar cells. Until now, succinonitrile has been used either with an ionic liquid [9–19], an organic iodide salt [13,14,20], an inorganic iodide salt [19], or with a polymer matrix [21–29] in the following composition: SN (with or without a polymer matrix)-XI-I_2. Here, the notation, X,

* Corresponding author.
E-mail address: rgupta@ksu.edu.sa (R.K. Gupta).

https://doi.org/10.1016/j.ssi.2018.10.008
Received 5 March 2018; Received in revised form 10 October 2018; Accepted 12 October 2018
Available online 16 October 2018
0167-2738/ © 2018 Elsevier B.V. All rights reserved.

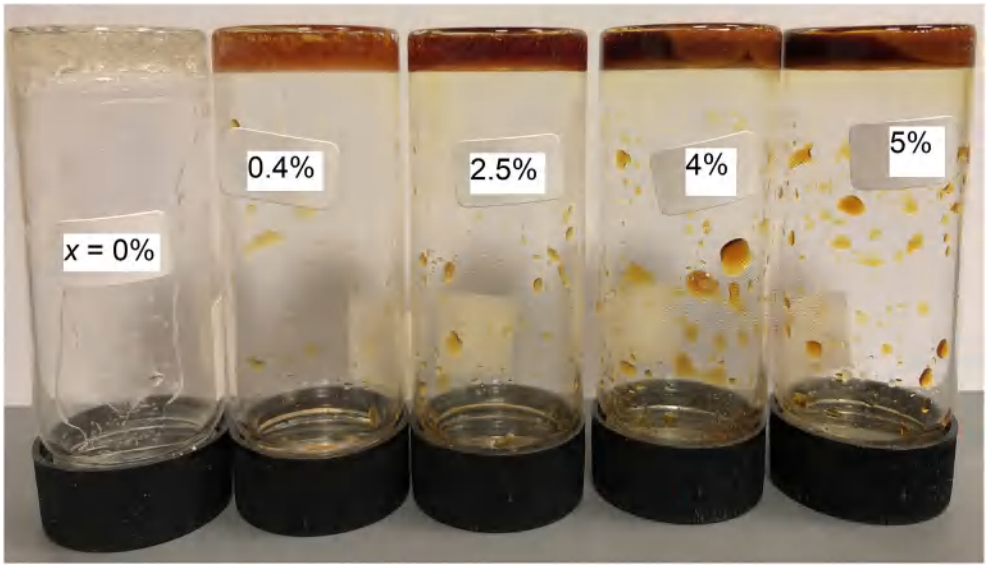

Fig. 1. SN-LiI-I_2 electrolytes (x = 0–5%) at room temperature (25 °C).

represents a cation of an ionic liquid, an organic salt, or an inorganic salt. Wang et al. [9] have used an ionic liquid, *N*-methyl-N-butylpyrrolidinium iodide to prepare a solid electrolyte, which exhibited $\sigma_{25°C}$ of 3.3×10^{-3} S cm^{-1}, apparent diffusion coefficients of 3.7×10^{-6} and 2.2×10^{-6} cm^2 s^{-1} for I^- and I_3^-, respectively, and η of 6.5% at 1 sun. Since then, numerous ionic liquids were used, which are as follows: *N*-dimethyl-N-propyl-N-butylammonium iodide [13], ethyl methyl imidazolium iodide [13], dimethyl imidazolium iodide [13], ethyl methyl pyrrolidinium iodide [13], 1-butyl-3-methylimidazolium tetrafluoroborate [14], 1-vinyl-3-methylimidazolium iodide [15], 1-vinyl-3-ethylimidazolium iodide [15], 1-vinyl-3-butylimidazolium iodide [15], 1-methyl-3-acetylimidazolium iodide [16], 1-ethyl-3-methylimidazolium iodide [16], 1-propyl-3-methylimidazolium iodide [16],1-methyl-3-propylimidazolium iodide (MPII) [17], 1-methyl-3-butylimidazolium iodide [17], 1-alkyl-2,3-dimethylimidazolium iodide [18], 1,2-dimethyl-3-propylimidazolium iodide [19], and 1-butyl-3-methylimidazolium iodide [19]. The WE structure was also modified by several research groups in order to improve the cell efficiency [10–12]. Dai et al. [13,20] thoroughly studied electrical, diffusion and thermal properties of tetrabutylammonium iodide (TBAI)-and tetraethylammonium iodide (TEAI)-based electrolytes. The former electrolyte exhibited better electrical conductivity and diffusion coefficients. The DSSC based on the TBAI electrolyte showed cell efficiency of 5% [14]. Gupta et al. [21–25] showed that a blend of SN and poly(ethylene oxide) in equal weight proportion can be used as a polymer matrix to prepare fast ion conducting solid electrolytes. In the blend-MI-I_2 (M = Li or K) electrolytes, the K^+ ions-based electrolyte exhibited better electrical conductivity than the Li^+ ions-based electrolyte; however, the later showed better photovoltaic properties [26]. Hwang et al. [27] prepared (SN-polyacrylonitrile)-1-propyl-2,3-dimethylimidazolium iodide-I_2-*N*-methyl benzimidazole electrolyte-based DSSC and reported cell efficiency of 3.3%. The efficiency was further improved to 7.6% by using a hierarchical structure of the WE [27]. Zhu et al. [28] showed cell efficiency of 4.4% using an (SN-neopentylglycol)-MPII-LiI-I_2-TBP electrolyte ($\sigma_{25°C} \sim 2.1 \times 10^{-3}$ S cm^{-1}). A (polyethylene glycol-SN-thiourea)-TiO_2-KI-I_2 electrolyte solution was also used in the DSSC, which exhibited η of 2.38% at 1 sun [29].

Byrne et al. [19] synthesized an SN-LiI-I_2 electrolyte in 100:5:1 mol ratio and fabricated a DSSC, which exhibited η of 3.58% at 1 sun. They used LiI because Li^+ ions are known to adsorb/interact well on/with the dye-sensitized TiO_2 layer, thereby they found an increase in electron injection rate and unfortunately a decrease in the TiO_2's conduction band edge [19,26]. However, they did not study the electrical, structural, and thermal properties of the SN-LiI-I_2 electrolyte. Therefore, in the present study, we have concentrated only on electrical, structural, and thermal properties of the SN-LiI-I_2 electrolyte. We have optimized the electrical conductivity ($\sigma_{25°C}$) of the SN-LiI-I_2 electrolytes via varying LiI-to-SN mole ratio (x) from 0 to 5%. The electrolytes with compositions, $x > 5\%$ were inhomogeneous in nature. The electrical conductivity is determined with temperature in order to determine the nature of ion transport and the activation energy. Ionic transference number (t_{ion}) is measured to determine the ionic contribution to the total electrical conductivity of the electrolyte. The electrical transport properties are explained using the vibrational spectroscopy study. We have also carried out the differential scanning calorimetry (DSC) for determining the melting temperature of the electrolytes exactly as suggested by the vibrational spectroscopy and $\log\sigma - T^{-1}$ studies.

2. Experimental details

2.1. Electrolyte preparation

Succinonitrile, LiI, and I_2, all from the Sigma-Aldrich chemicals, were used without further purification. A mixture of succinonitrile, LiI, and I_2 in a glass vial was first kept at ~70 °C in an oven for a few minutes to melt the succinonitrile and then stirred at ~60 °C for 24 h, which resulted in a homogeneous redox-couple electrolyte. The LiI-to-succinonitrile mole ratio (x) was varied from 0 to 5%. The I_2-to-LiI mole ratio was kept equal to 10%. As shown in Fig. 1, the electrolytes were solid at room temperature.

2.2. Electrolyte characterizations

For the electrical conductivity measurement, the melted electrolyte solution was poured at the 0.5-mm thick space between platinum electrode plates (active area ~16 mm^2) of a specially designed sample holder kept at ~70 °C in an oven. The sample holder is shown in Fig. 2. After cooling at room temperature, a complex impedance curve was acquired in a frequency range of 10–10^5 Hz with ac amplitude of 20-mV using a HIOKI IM 3533-01 LCR meter. The electrical conductivity was calculated using an expression, $\sigma = t/(a\,R)$, where t is spacing between platinum electrode plates, a is an active area of electrode plates, and R is a resistance of the complex impedance curve intersecting at the real axis. For the $\log \sigma - T^{-1}$ study, the sample holder was kept in a digitally temperature-controlled oven. The actual electrolyte temperature was determined using a digital thermometer attached to the sample

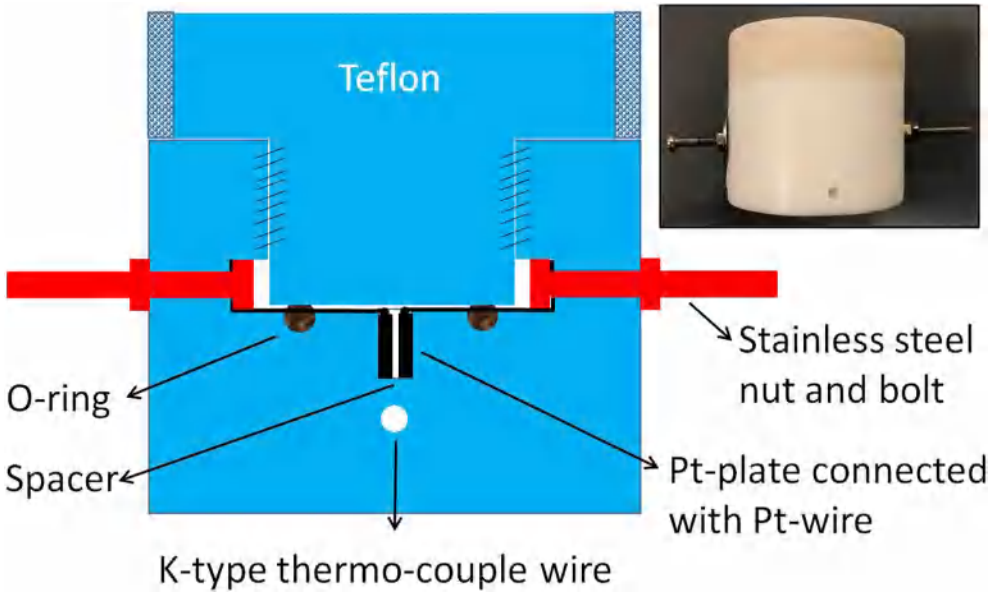

Fig. 2. Schematic view of a Teflon-based sample holder (inset).

holder through a K-type thermocouple.

Ionic transference number (t_{ion}) was determined using a dc polarization method utilizing a blocking electrode, e.g., platinum plate and is similar to the Wagner's dc polarization technique [30–32]. In this method, the melted electrolyte solution was poured at the 0.5-mm thick space between platinum plates (blocking electrode) of the sample holder kept at ~70 °C in an oven. It was then left to cool at room temperature. A dc potential of ~0.25 V was applied across the electrodes and the dc current flowing through the circuit was monitored using a Keithley 2000 multimeter at t ~ 0 s for total current (I_T) and at ~24 h for residual current (I_e). Subsequently, ionic transference number was determined using the formula, $t_{ion} = 1 - (I_e/I_T)$. The ratio, I_e/I_T corresponds to the electronic transference number (t_e).

Raman spectra of the electrolytes were collected from 45 cm^{-1} to 4000 cm^{-1} with a resolution of 1 cm^{-1} using a JASCO's NRS-4500 Confocal Raman Microscope. The Raman microscope used a laser beam of 532.07 nm. The Fourier-transform infrared (FT-IR) spectrum of the electrolyte was measured in the range of 400–4000 cm^{-1} with a resolution of 2 cm^{-1} using an IRPrestige-21 spectrometer (Shimadzu, Japan). It was carried out using a ~0.25-mm thick pellet consisting of KBr powder and the electrolyte. The heat flow of the electrolyte was measured by a differential scanning calorimeter (DSC-60A, Shimadzu, Japan) under a nitrogen gas atmosphere with 10 °C min^{-1} heating rate and in the range of −50 °C to 70 °C.

3. Results and discussion

3.1. Electrical properties

Fig. 3 shows the $\sigma_{25°C} - x$ curve of the SN-LiI-I_2 electrolytes, where LiI to succinonitrile mole ratio (x) varied from 0 to 5%; while, the I_2 to LiI mole ratio was set at 10%. Being a non-ionic material, $\sigma_{25°C}$-value of the succinonitrile should be quite low [21]; however, we achieved a $\sigma_{25°C}$-value of ~10^{-7} S cm^{-1} as observed earlier by Long et al. [6,7]. The availability of residuals in the pure succinonitrile can be ascribed for the higher $\sigma_{25°C}$-value [6,7]. As mentioned earlier, the plastic phase of the pure succinonitrile involves trans-gauche isomerization of the molecules and molecular jumps from one diagonal position of the body-centred cubic (bcc) structure to another [8]. The trans isomers act as "impurities" that create mono-vacancies in the bcc lattice and lead to high molecular diffusivity [33]. Therefore, the residuals in the ionic form are easily transported in the plastic phase environment resulting

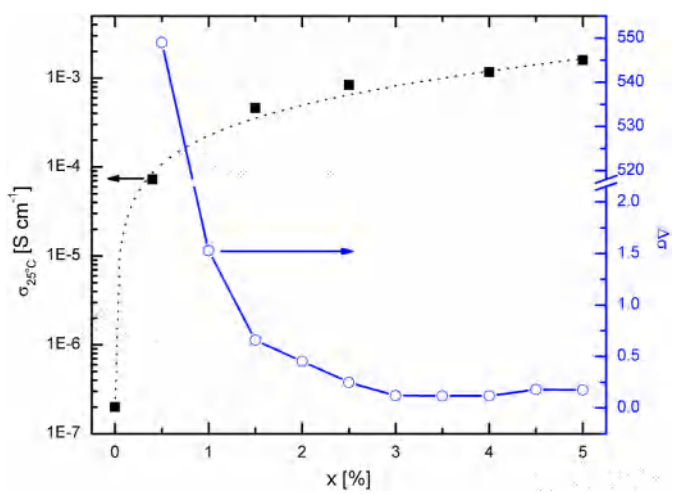

Fig. 3. Composition (x) dependent $\sigma_{25°C}$ and relative conductivity enhancement factor ($\Delta\sigma$) of the SN-LiI-I_2 electrolytes (x = 0–5%). The line guides the eye.

in the higher $\sigma_{25°C}$-value. This also led to a huge increase in the $\sigma_{25°C}$-value for a small fraction of LiI-I_2 mixture (x = 0.4%). Further increase in x up to 5% led to an increase in the $\sigma_{25°C}$-value. The $\sigma_{25°C} - x$ curve followed an exponential rise–type behavior. The electrolytes with x > 5% exhibited inhomogeneity. This later is due to low Gutmann donor number of the nitrile group of the succinonitrile, with a consequence of a lesser tendency to 'solvate' cations [8]. Therefore, the electrolyte with x = 5% is referred to as the optimum conducting composition (OCC), and possesses the highest value of electrical conductivity (~1.6×10^{-3} S cm^{-1}) at 25 °C. We calculated the relative conductivity enhancement factor, $\Delta\sigma = [\sigma_x - \sigma_{x-0.05}]/\sigma_{x-0.05}$ [34] using the extrapolated $\sigma_{25°C} - x$ data and showed it in the Fig. 3. It portrayed a fast decrease in the $\Delta\sigma$-value from 549 (x = 0.5%) to 0.25 (x = 2.5%) and then nearly a flat $\Delta\sigma$-value of ~0.15 thereafter.

The variations of $\sigma_{25°C}$ and $\Delta\sigma$ with x can be explained using a well-known expression of electrical conductivity, $\sigma = nq\mu$, where n, q, and μ are the concentration, charge, and mobility of the free ionic species, respectively [3,35]. This expression involves the following three competitive processes: (i) dissociation of the LiI by the succinonitrile resulting in free Li^+ and I^- ions, and consequently, free I_3^- ions [6–8,13,20,34,36]; (ii) the Coulombic interactions between the Li^+ and

I^- ions [34,36], and (iii) the ions interaction with the polar ends of the succinonitrile molecules, which can not only hinder the ion motion but also affect the trans-gauche isomerisation process [7,8,37–41]. The change in the isomerisation process may lead to an increased number of vacancies and hence higher molecular diffusivity [33]. Long et al. [6,7] observed higher diffusivity for succinonitrile molecules than the anions and cations. They also noticed higher molecular diffusivity and hence higher mobility after the melting temperature of the electrolytes. It is also worth mentioning that being uncharged, an ion-pair formation leads to higher mobility in the electrolyte [34]. Therefore, the processes (i) and (ii) control the concentration of the free ionic species; while, the processes (ii) and (iii) control the ionic mobility. For the present electrolytes, one can expect a dominance of the process (i) at $x = 0.4\%$ resulting in a huge rise of the $\sigma_{25^\circ C}$-value with the highest $\Delta\sigma$-value. The process (i) is still dominated at $x = 1.5\%$; however, the processes (ii) and (iii) started to act. From $x = 2.5\%$ onwards all of the processes played a role in the conductivity enhancement; however, the dominance of the processes (ii) and (iii) is indicated by nearly flat region of the $\Delta\sigma$-value. This assertion was supported by the $\log\sigma - T^{-1}$, the vibrational spectroscopy and the differential scanning calorimetry studies, and have been discussed below.

The temperature dependent electrical conductivity study is essential to identify the nature of ion transport and to evaluate the activation energy (E_a) of the electrolyte [3,34,35]. Fig. 4 exhibits $\log\sigma - T^{-1}$ plots of the SN-LiI-I_2 electrolytes, where x varied from 0 to 5%. The pure succinonitrile ($x = 0$) depicted a linear increase in log σ-value with T^{-1} in regions – I and II, and is similar to those reported earlier [6,7]. The linear trend indicated that the pure succinonitrile is a homogeneous system and as indicated by the ionic transference number measurement majority of migrating charge carriers of the residuals are in ionic form. The electrolytes with $x = 0.4$–5% exhibited a similar trend and the conductivity enhancement occurred in both regions. The linear trend can be expressed using an Arrhenius equation: $\sigma = \sigma_o \exp[-E_a/k_B T]$, where σ_o is a pre-exponential factor and k_B is the Boltzmann constant [3,34,35]. The slope of the $\log\sigma - T^{-1}$ plot resulted in activation energy (E_a), which is shown in Fig. 5 for temperature regions, I and II. The value of E_a increased with increasing value of x in both the regions. However, E_a-value was relatively low in the region – II, where the electrolytes are in the liquid form. This indicates an easy ion transport in the region – II. The increase in E_a-value with increasing x indicates the dominance of the processes (ii) and (iii) over the process (i). It is contrary to commonly observed study for the poly(ethylene oxide)-succinonitrile *blend*-based polymer electrolytes, where the value of E_a was decreased with increasing x up to the OCC and then increased [22–24,34]. For these polymer electrolytes, the value of n was increased up to the OCC only; while, the value of μ was continuously increased due to the plasticizing effect of the succinonitrile and the salt.

In an I^-/I_3^- redox-couple-based electrolyte having a metal salt MI, I^-, I_3^-, and M^+ ions are present as charge carriers and contribute to the electrical conductivity of the electrolyte [2,3,5,26,36]. Kalaignan et al. [36] observed ionic transference number close to unity for the PEO-KI-I_2 electrolyte and showed K^+ ions along with I^-/I_3^- redox-couple as charge carriers. We, therefore, measured ionic (t_{ion}) and electronic (t_e) transference numbers of the SN-LiI-I_2 electrolytes ($x = 0$–5%) at room temperature and showed in Fig. 6. Pure succinonitrile ($x = 0$) exhibited t_{ion} ~0.92 and t_e ~0.08 indicating that residuals present in the succinonitrile contribute significantly in ionic form and result in electrical conductivity of ~10^{-7} S cm^{-1} at room temperature. The electrolyte with $x = 0.4\%$ possessed t_{ion} ~0.94 and t_e ~0.06. Further increase in x with 2.5% enhanced t_{ion}-value to ~0.97 and reduced t_e-value to ~0.03. For the electrolytes with $x = 4$ and 5%, we measured t_{ion} ~0.98 and t_e ~0.02. This study indicated ions as predominant charge carriers and the ionic contribution to the electrical conductivity increased with increasing x-value.

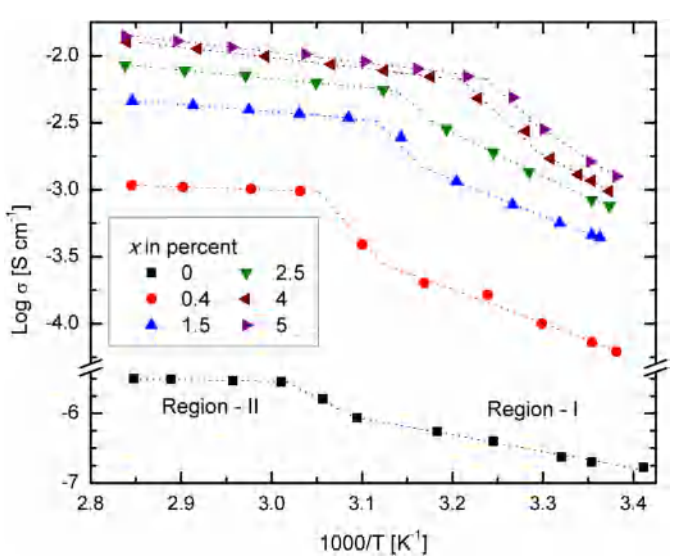

Fig. 4. $\log\sigma - T^{-1}$ plots of the SN-LiI-I_2 electrolytes ($x = 0$–5%).

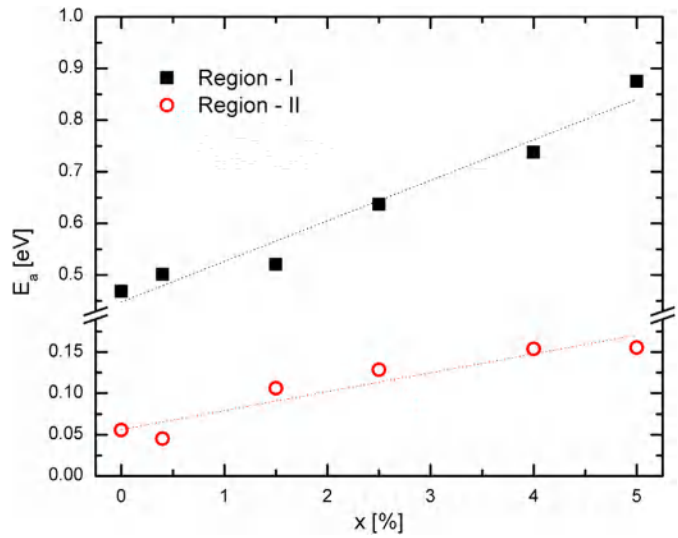

Fig. 5. Activation energy (E_a) of the SN-LiI-I_2 electrolytes ($x = 0$–5%) for temperature regions, I and II.

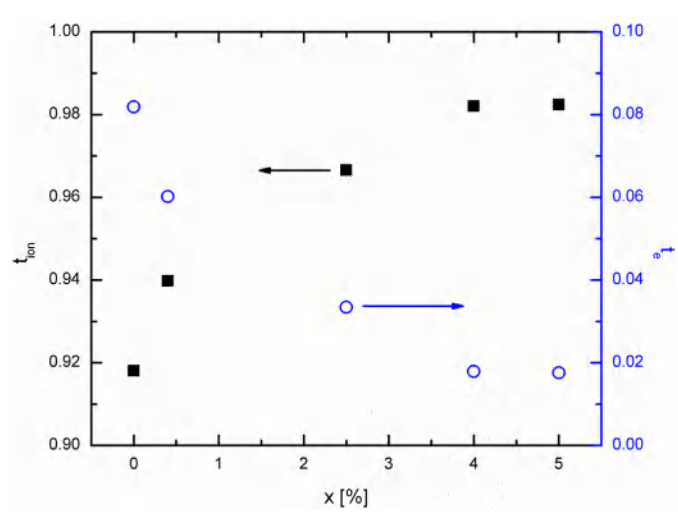

Fig. 6. Ionic (t_{ion}) and electronic (t_e) transference numbers of the SN-LiI-I_2 electrolytes ($x = 0$–5%) at room temperature.

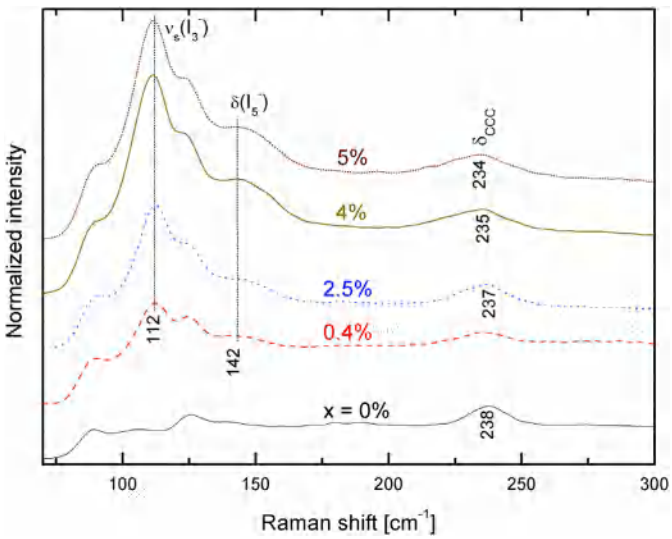

Fig. 7. Raman spectra of the SN-LiI-I_2 electrolytes (x = 0–5%).

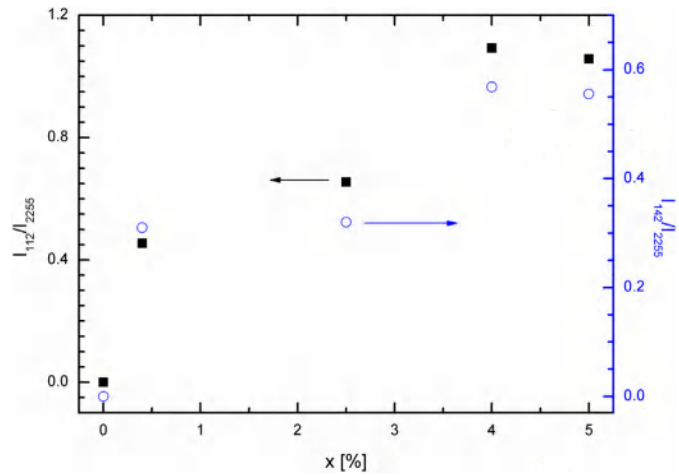

Fig. 8. Relative intensities estimated from the Raman spectra of the SN-LiI-I_2 electrolytes (x = 0–5%).

3.2. Structural properties

In the presence of an alkali salt MI, I_2 transforms into I_3^- using a reaction: $I_2 + I_{MI}^- \rightarrow I_3^-$, which gets reduced to I^- at the counter electrode [36,42,43]. The presence of I_2 and I_3^- were monitored using the Raman spectroscopy [36,42,43]. One can also expect formation of a small fraction of poly-iodide ions using a reaction: $I_2 + I_3^- \rightarrow I_5^-$, which are not useful for the DSSC operation [2,3]. Therefore, we carried out Raman spectroscopy study at room temperature and Raman spectra of the SN-LiI-I_2 electrolytes (x = 0–5%) in the range of 70–300 cm^{-1} are portrayed in Fig. 7. Pure succinonitrile (x = 0) showed a Raman spectrum similar to that reported by Fengler and Ruoff [44]. We, therefore, assigned the observed vibrational frequency at 238 cm^{-1} as a bending mode (δ_{CCC}). The electrolytes with x = 0.4–5% showed a similar δ_{CCC}-peak, however, with a slight shift towards lower frequency most probably due to softening of C—C chains of the succinonitrile as indicated by the FT-IR spectroscopy and DSC studies, which have been discussed later. We also observed a new peak at ~112 cm^{-1} for the electrolytes with x = 0.4–5%. This peak corresponds to stretching (ν) mode of tri-iodide ions [36,42,43]. The electrolytes with x = 0.4–5% also exhibited a broad peak at ~142 cm^{-1} and corresponds to bending (δ) mode of a poly-iodide ions such as I_5^- [36,42,43]. The intensities of the $\nu(I_3^-)$- and $\delta(I_5^-)$-modes increased with increasing x-value, and their relative intensities with respect to the very strong peak of the $\nu_{C\equiv N}$ at 2255 cm^{-1} [44] are shown in Fig. 8 for direct visualization. The electrolytes with x = 4% and 5% showed nearly equal values of the relative intensities of the $\nu(I_3^-)$- and $\delta(I_5^-)$-modes indicating a saturation condition of the tri-iodide and poly-iodide ions formation. Fig. 8 also indicates formation of a small fraction of poly-iodide ions relative to the tri-iodide ions. It is also worth mentioning that we did not get a peak at ~180 cm^{-1} corresponding to aggregated iodine and a peak at ~212 cm^{-1} due to isolated iodine in the Raman spectra of the electrolytes [36,42]. This indicates a complete conversion of added I_2 into I_3^- ions.

A conformational change of a polymer can easily be detected using the FT-IR spectroscopy [45]. We, therefore, acquired FT-IR spectra of the SN-LiI-I_2 electrolytes (x = 0–5%), which are showed in Fig. 9(a) and (b) in the ranges of 400–1550 cm^{-1} and 2100–3200 cm^{-1}, respectively. The pure succinonitrile (x = 0) possessing a regular conformation and packing of the chains in the plastic crystal phase, resulted in well-defined and sharp bands in the FT-IR spectrum. The spectrum is also similar to that reported by Fengler and Ruoff [44]. We, therefore, assigned the observed frequencies accordingly and marked in the Fig. 9(a) and (b). In the figures, the notations are as follows: ν, stretching; δ, bending; ω, wagging; t, twisting; and ρ, rocking modes. An increase of x from 0.4% to 5% did not shift the position of the modes; however, it resulted in a band broadening. The band broadening indicates amorphous phase formation due to molecular chain disorder [45]. The broadening is more visible at 1426 cm^{-1} (δ_{CH2} mode), 2254 cm^{-1} ($\nu_{C\equiv N}$ mode), and ~3000 cm^{-1} (ν_{CH2} modes). The ν_{CH2} modes comprise symmetric mode at ~2952 cm^{-1} and asymmetric mode at 2988 cm^{-1}. We, therefore, estimated relative area, which is equal to $(A_x - A_0)/A_0$ with x = 0–5%, at 1426 cm^{-1}, 2254 cm^{-1}, and ~3000 cm^{-1}, and showed in Fig. 10. This portrayed an increase of relative area with increasing x for the δ_{CH2}, $\nu_{C\equiv N}$, and ν_{CH2} modes indicating an increase of the amorphicity with increasing x. This is corroborating well the DSC study and the conjecture proposed by Alarco et al. [8] and Chen et al. [17], which have been discussed in the next section.

The electrolytes also exhibited a splitting of the $\nu_{C\equiv N}$ mode at ~2254 cm^{-1}, which is more pronounced for the higher values of x (2.5–5%). It is most probably due to the interaction of the cyano radical of the succinonitrile with the tri-iodide ions [37–41,45]. This not only hindered the ion motion but also affected the trans-gauche isomerisation process as indicated by an increase in σ- and E_a-values with increasing x. In the FT-IR spectra of the electrolytes (x = 0.4–5%), we did not get a peak nearly at 433 cm^{-1} corresponding to the isolated or aggregated LiI molecules [46]. This suggested a complete salvation of the LiI by the succinonitrile, which resulted in free Li^+ ions with I^-/I_3^- redox-couple.

3.3. Thermal property

Fig. 4 exhibited a mid-region between the temperature regions I and II in the $\log\sigma - T^{-1}$ plots, which is a region in the DSC thermogram starting from the onset of the endothermic T_m-peak of the electrolyte [6–8]. We observed a shift in the mid-region to lower temperature with increasing x, which suggests a decrease of the melting temperature with x [17]. Therefore, we determined the melting temperature of the SN-LiI-I_2 electrolytes (x = 0, 2.5 and 5%) exactly using a differential scanning calorimeter and the DSC curves are shown in Fig. 11. Being a plastic crystal, succinonitrile (x = 0) showed a strong endothermic peak at 57.7 °C, which is similar to those reported earlier [6–8] and corresponds to the melting temperature (T_m). The peak area corresponds to the heat of enthalpy. The electrolyte with x = 2.5% exhibited a reduced T_m-peak at 55.6 °C; while, two very weak T_m-peaks at 37.1 °C and 48.1 °C were observed for the electrolyte with x = 5% (OCC). The T_m-peak area was also reduced with increasing x. A strong endothermic T_{pc}-peak at −38.4 °C was observed for the pure succinonitrile, which was

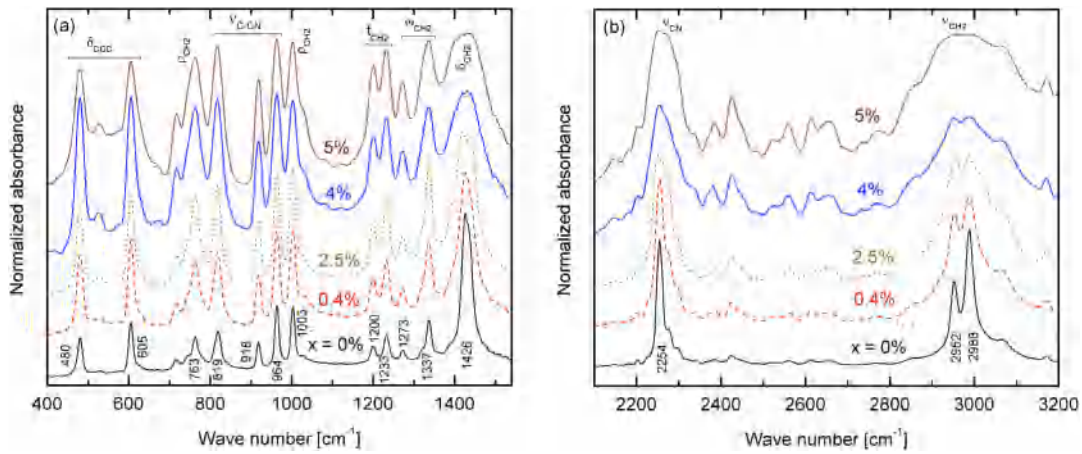

Fig. 9. FT-IR spectra of the SN-LiI-I_2 electrolytes (x = 0–5%).

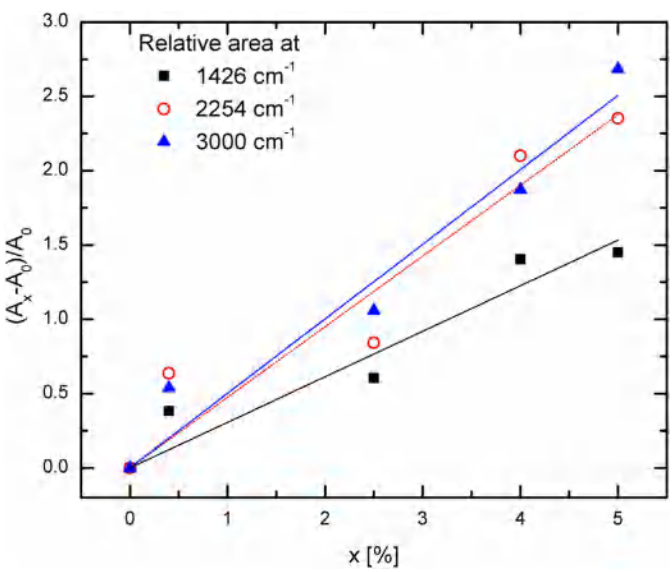

Fig. 10. Relative area estimated from the FT-IR spectra of the SN-LiI-I_2 electrolytes (x = 0–5%).

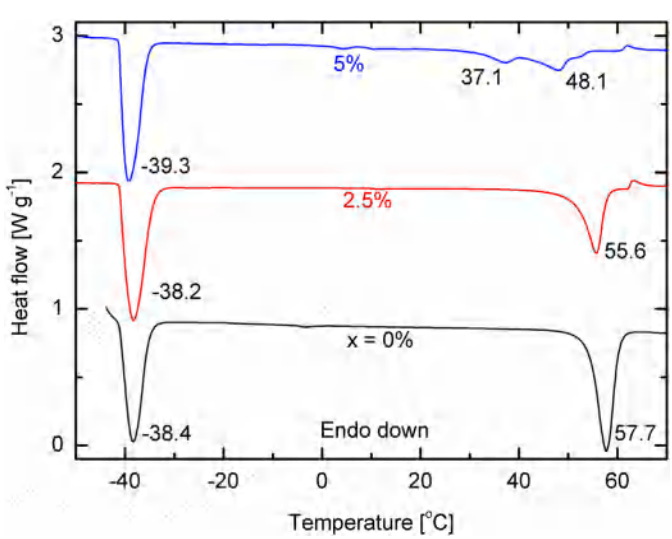

Fig. 11. DSC curves of the SN-LiI-I_2 electrolytes (x = 0, 2.5 and 5%).

almost unaffected for the electrolytes with x = 2.5 and 5%. A number of SN-LiY electrolytes, where Y stands for an anion, exhibited similar phenomena, i.e., a decrease in area and position of the T_m-peak and nearly unaffected T_{pc}-peak [6–8]. The (SN-ionic liquid)-$LiClO_4$-I_2 electrolytes also showed similar phenomena with increasing $LiClO_4$ concentration [17]. Alarco et al. [8] and Chen et al. [17] proposed formation of a 'succinonitrile-salt' solid solution and a liquid eutectic phase in the SN-LiY electrolytes. The 'succinonitrile-salt' solid solution contains free ions in the plastic crystal phase, which creates highly conductive disordered domains. In the present case, we observed an increase in amorphicity with increasing x through the conformation change of the succinonitrile as indicated by a red shift in the δ_{CCC}-band, and broadening in δ_{CH2}-, $\nu_{C\equiv N}$-, and ν_{CH2}-bands. The amorphicity is the highest for the OCC as indicated by the existence of the binary very weak T_m-peaks at 37.1 °C and 48.1 °C. This suggests availability of a large number of free ions with interactions resulting in the highest $\sigma_{25°C}$- and E_a-values of the OCC.

4. Conclusions

A plastic crystal-based solid electrolyte, succinonitrile-LiI-I_2 was prepared with varying LiI-to-succinonitrile mole ratio (x) from 0 to 5% and I_2-to-LiI mole ratio set for 10%. The electrical conductivity ($\sigma_{25°C}$) and the relative conductivity enhancement factor showed an exponential-type rise and fall, respectively, with increasing x and was explained using the free ion generation and the interaction phenomena by the vibrational spectroscopy study. The electrolyte with x = 5% exhibited the highest $\sigma_{25°C}$-value (OCC). The electrolytes exhibited an increase in activation energy with increasing x most probably due to an increase in interaction between the cyano redicals of the succinonitrile and tri-iodide ions. The DSC showed a decrease of area and position of the melting temperature peak with increasing x revealing an increase in the highly conductive disordered domains with increasing x.

Acknowledgement

The authors extend their appreciation to the College of Applied Medical Sciences Research Center and the Deanship of Scientific Research at King Saud University for funding this research.

References

[1] A. Luque, S. Hegedus, Handbook of Photovoltaic Science and Engineering, John Wiley & Sons, Ltd., United Kingdom, 2011.
[2] A. Hagfeldt, G. Boschloo, L.C. Sun, L. Kloo, H. Pettersson, Chem. Rev. 110 (11) (2010) 6595.
[3] J.H. Wu, Z. Lan, J.M. Lin, M.L. Huang, Y.F. Huang, L.Q. Fan, G.G. Luo, Chem. Rev. 115 (5) (2015) 2136.

[4] Y. Chiba, A. Islam, Y. Watanabe, R. Komiya, N. Koide, L.Y. Han, Jpn. J. Appl. Phys. 2 Lett. Express Lett. 45 (24–28) (2006) L638.
[5] B. Li, L.D. Wang, B.N. Kang, P. Wang, Y. Qiu, Sol. Energy Mater. Sol. Cells 90 (5) (2006) 549.
[6] S. Long, D.R. MacFarlane, M. Forsyth, Solid State Ionics 161 (1–2) (2003) 105.
[7] S. Long, D.R. MacFarlane, M. Forsyth, Solid State Ionics 175 (1–4) (2004) 733.
[8] P.J. Alarco, Y. Abu-Lebdeh, A. Abouimrane, M. Armand, Nat. Mater. 3 (7) (2004) 476.
[9] P. Wang, Q. Dai, S.M. Zakeeruddin, M. Forsyth, D.R. MacFarlane, M. Gratzel, J. Am. Chem. Soc. 126 (42) (2004) 13590.
[10] B. Lee, D.B. Buchholz, P.J. Guo, D.K. Hwang, R.P.H. Chang, J. Phys. Chem. C 115 (19) (2011) 9787.
[11] D.K. Hwang, B. Lee, D.H. Kim, RSC Adv. 3 (9) (2013) 3017.
[12] D. Xu, C.Z. Shi, L. Wang, L.H. Qiu, F. Yan, J. Mater. Chem. A 2 (25) (2014) 9803.
[13] Q. Dai, D.R. MacFarlane, M. Forsyth, Solid State Ionics 177 (3–4) (2006) 395.
[14] Z.G. Chen, H. Yang, X.H. Li, F.Y. Li, T. Yi, C.H. Huang, J. Mater. Chem. 17 (16) (2007) 1602.
[15] Y. Jiang, Y.L. Cao, P. Liu, J.F. Qian, H.X. Yang, Electrochim. Acta 55 (22) (2010) 6415.
[16] X.M. Huang, D. Qin, X.L. Zhang, Y.H. Luo, S.Q. Huang, D.M. Li, Q.B. Meng, RSC Adv. 3 (19) (2013) 6922.
[17] J.N. Chen, T.Y. Peng, K. Fan, R.J. Li, J.B. Xia, Electrochim. Acta 94 (2013) 1.
[18] D. Hwang, D.Y. Kim, S.M. Jo, V. Armel, D.R. MacFarlane, D. Kim, S.Y. Jang, Sci. Rep. 3 (2013) 1.
[19] O. Byrne, A. Coughlan, P.K. Surolia, K.R. Thampi, Prog. Photovolt. 23 (4) (2015) 417.
[20] Q. Dai, D.R. MacFarlane, P.C. Howlett, M. Forsyth, Angew. Chem. Int. Ed. 44 (2) (2005) 313.
[21] R.K. Gupta, H.M. Kim, H.W. Rhee, J. Phys. D. Appl. Phys. 44 (20) (2011) 205106.
[22] R.K. Gupta, H.W. Rhee, Adv. OptoElectron. 2011 (2011) 102932.
[23] R.K. Gupta, H.W. Rhee, Electrochim. Acta 76 (2012) 159.
[24] R.K. Gupta, H.W. Rhee, J. Phys. Chem. B 117 (24) (2013) 7465.
[25] R.K. Gupta, I.M. Bedja, Phys. Status Solidi (a) 211 (7) (2014) 1601.
[26] R.K. Gupta, I. Bedja, J. Phys. D. Appl. Phys. 50 (24) (2017) 245501.
[27] D. Hwang, D.Y. Kim, S.Y. Jang, D. Kim, J. Mater. Chem. A 1 (4) (2013) 1228.
[28] X.M. Zhu, Y.Y. Gui, Y. Jiang, X.P. Ai, H.X. Yang, Y.L. Cao, Electrochim. Acta 147 (2014) 535.
[29] H. Jauhari, R. Grover, O. Nanda, K. Saxena, RSC Adv. 6 (71) (2016) 66788.
[30] J.B. Wagner, C. Wagner, J. Chem. Phys. 26 (6) (1957) 1597.
[31] R.C. Agrawal, K. Kathal, R.K. Gupta, Solid State Ionics 74 (3–4) (1994) 137.
[32] R.C. Agrawal, R. Kumar, R.K. Gupta, Mater. Sci. Eng. B 57 (1) (1998) 46.
[33] H.M. Hawthorne, J.N. Sherwood, Trans. Faraday Soc. 66 (1970) 1792.
[34] R.K. Gupta, H.W. Rhee, Bull. Kor. Chem. Soc. 38 (3) (2017) 356.
[35] R.C. Agrawal, R.K. Gupta, J. Mater. Sci. 34 (6) (1999) 1131.
[36] G.P. Kalaignan, M.S. Kang, Y.S. Kang, Solid State Ionics 177 (11–12) (2006) 1091.
[37] G. Cardini, R. Righini, S. Califano, J. Chem. Phys. 95 (1) (1991) 679.
[38] P. Derollez, J. Lefebvre, M. Descamps, W. Press, H. Fontaine, J. Phys. Condens. Matter 2 (33) (1990) 6893.
[39] I. Matsubara, J.H. Magill, Polymer 7 (1966) 199.
[40] J. Maillo, P. Pages, E. Vallejo, T. Lacorte, J. Gacén, Eur. Polym. J. 41 (4) (2005) 753.
[41] X. Li, A. Reynal, P. Barnes, R. Humphry-Baker, S.M. Zakeeruddin, F. De Angelis, B.C. O'Regan, Phys. Chem. Chem. Phys. 14 (44) (2012) 15421.
[42] L. Andrews, E.S. Prochaska, A. Loewenschuss, Inorg. Chem. 19 (2) (1980) 463.
[43] K.R. Loos, A.C. Jones, J. Phys. Chem. 78 (22) (1974) 2306.
[44] O.I. Fengler, A. Ruoff, Spectrochim. Acta A Mol. Biomol. Spectrosc. 57 (1) (2001) 105.
[45] C. Castiglioni, N.J. Everall, J.M. Chalmers, P.R. Griffiths (Eds.), Vibrational Spectroscopy of Polymers: Principles and Practice, John Wiley & Sons, Chichester, 2007.
[46] K. Nakamoto, Infrared and Raman Spectra of Inorganic and Coordination Compounds: Part A: Theory and Applications in Inorganic Chemistry, John Wiley & Sons, NJ, 2008, p. 156.